

Perspective Multiplication for Multi-Perspective Enrolment in Finger Vein Recognition

Bernhard Prommegger¹, Andreas Uhl¹

Abstract: Finger vein recognition deals with the identification of subjects based on their venous pattern within the fingers. It has been shown that its recognition accuracy heavily depends on a good alignment of the acquired samples. There are several approaches that try to reduce the impact of finger misplacement. However, none of these approaches is able to prevent all possible types of finger misplacements. As finger vein scanners are evolving towards contact-less acquisition, alignment problems, especially due to longitudinal finger rotation, are becoming even more important. One way to tackle this problem is capturing the vein structure from different perspectives during enrolment, but cost and complexity of capturing devices increases with the number of involved cameras. In this article, a new method to reduce the number of cameras needed for multi-perspective enrolment is presented. The reduction is achieved by introducing additional pseudo perspectives in-between two adjacent cameras. The obtained perspectives are used for additional comparisons during authentication. This way, the complexity of the enrolment devices can be reduced while keeping the recognition performance at a high level.

Keywords: Finger Vein Recognition, Longitudinal Finger Rotation, Multi-Perspective Enrolment, Perspective Multiplication.

1 Introduction

Vascular pattern based biometric systems, commonly denoted as vein biometrics, offer several advantages over other well-established biometric recognition systems. In particular, hand and finger vein systems have become a serious alternative to fingerprint based ones for several applications. Vein based systems use the structure of the blood vessels inside the human body, which becomes visible under near-infrared (NIR) light. As the vein structure is located inside the human body, it is resistant to abrasion and external influences on the skin. Furthermore, a liveness detection to detect presentation attacks can be performed easily [KZ12].

The performance of finger vein recognition systems suffers from different internal and external factors. Internal factors include the design and configuration of the sensor itself, especially the NIR light source and the camera module. External factors include environmental conditions (e.g. temperature and humidity) and deformations due to misplacement of the finger, typically including shifts, tilt, bending and longitudinal rotation. Several publications addressed that such finger misplacements cause degradations in the performance of recognition systems: The need for a robust finger vein image normalisation including rotational alignment has already been mentioned by Kumar and Zhou in

¹ Department of Computer Sciences, University of Salzburg, AUSTRIA, {bprommeg, uhl}@cs.sbg.ac.at

2012 [KZ12]. Chen *et al.* [Ch18] state that deformation correction can be done either during pre-processing, feature extraction or comparison. Moreover, the physical design of the sensor, e.g. as proposed by Kauba *et al.* [KPU18], can help to avoid misplacements of the finger. In [PKU18a] the authors showed, that longitudinal finger rotation has a severe influence on the recognition performance of a finger vein recognition system. There are several approaches that try to reduce the influence of these issues during the processing of the vein patterns, e.g. [Ch18, Hu10, KZ12, LLP09, Ma16, Pr19, Ya17]. Prommegger and Uhl [PU19] introduced two methods that make finger vein recognition invariant against longitudinal rotation. Both methods acquire multiple perspectives during enrolment, while actual authentication is done with traditional single-perspective acquisition. The first approach, multi-perspective enrolment (MPE), compares the probe image to all acquired enrolment perspectives, while the second approach, perspective cumulative finger vein templates, generates a single template that contains the vein pattern all around the finger. As finger vein systems evolve towards contact-less operation, problems resulting from finger misplacements, e.g. longitudinal rotation, will receive more attention in the future.

The main contribution of this work is the proposal of a method, perspective multiplication for multi-perspective enrolment (PM-MPE), to reduce the complexity and cost of the capturing device needed for multi-perspective enrolment for finger vein recognition. By combining MPE with the fixed angle method from [Pr19], the number of perspectives needed during enrolment of subjects is effectively reduced while the recognition performance is kept on a high level. The experiments are carried out using the *PLUSVein finger rotation data set* (PLUSVein-FR) [PKU18b]. To show the effectiveness of the proposed approach, its recognition results are compared to the results of original the MPE approach in [PU19].

The remainder of this paper is organized as follows: In section 2 the proposed method for reducing the perspectives acquired during enrolment is described. The experimental set-up together with its results are described in Section 3. Section 4 concludes the paper along with an outlook on future work.

2 Perspective Multiplication for Multi-Perspective Enrolment

MPE, as proposed in [PU19], requires the acquisition of multiple perspectives during enrolment. The angles of the different perspectives are linearly spaced over the desired acquisition range. For authentication, only a single perspective is acquired and compared to all enrolment samples together with a maximum rule score level fusion. If enough cameras are used during enrolment, negative effects of longitudinal finger rotation on the recognition performance can be inhibited. The invariance against longitudinal rotation is achieved by increasing the effort during enrolment (acquiring additional perspectives, feature extraction) and comparison (multi-perspective comparison). Additionally to the acquisition of multiple perspectives also circular pattern normalization (CPN, [PU19]), which essentially corresponds to a rolling of the finger assuming a circular finger shape, is applied.

It has been shown that rotation compensation can effectively improve the recognition performance, e.g. [Ch18, Hu10, LLP09, Ma16, Pr19, Ya17]. Prommegger *et al.* [Pr19] pro-

posed an approach that rotates the enrolled image by an pre-defined angle and compare the probe sample against all three versions: the original and the two rotated ones. This method improves the range, in which well performing vein pattern based recognition schemes achieve reasonable recognition results, from approximately $\pm 15^\circ$ to nearly $\pm 30^\circ$. Perspective multiplication for multi-perspective enrolment (PM-MPE), which is introduced in this paper, uses this knowledge to reduce the number of perspectives needed for MPE. During enrolment n perspectives with a rotational distance of α are acquired. PM-MPE adds two pseudo perspectives between two adjacent cameras by rotating every perspective with an rotational angle of $\pm\varphi = 1/3\alpha$ in both directions, where α is the rotational distance between two cameras. For authentication, as for traditional single-perspective finger vein recognition schemes, only a single perspective is acquired and compared to all enrolled perspectives and the generated pseudo perspectives. This leads to $3 * n$ comparisons for each authentication attempt. Fig. 1 shows this principle for a distance of 30° between two perspectives. On the left side, the MPE approach is visualized. It needs 12 cameras linearly spaced over the whole circle. On the right side the PM-MPE setup is visualized. It needs only four cameras (solid blue dots) positioned at 0° , 90° , 180° and 270° . The remaining perspectives (red circles) are generated by rotating the acquired finger vein images by a rotation angle of $\varphi = 30^\circ$ in both directions.

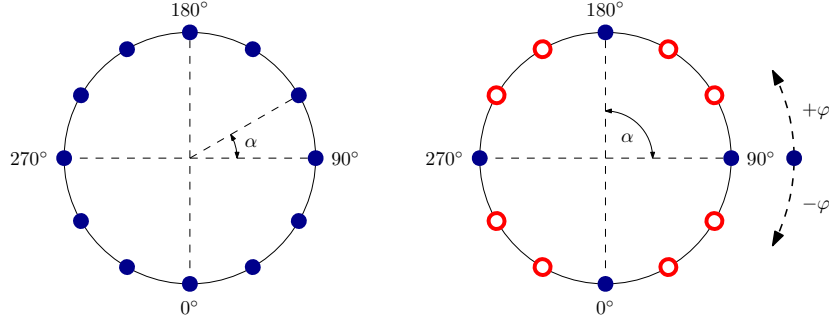


Fig. 1: Camera positioning for MPE (left) and PM-MPE (right) for a rotational distance of 30° between the perspectives. The filled blue dots are cameras, the red circles represent rotated perspectives.

MPE and PM-MPE are evaluated using vein pattern based features in combination with a correlation based comparison where the score is calculated between the input images and in horizontal and vertical direction shifted and rotated versions of the reference image as described in [MNM04]. The number of pixels shifted up and down (vertical shift) during the comparison depends on the angular range acquired during enrolment Θ (when enrolling the whole finger $\Theta = 360^\circ$), the number n of cameras involved and the height h of the extracted ROIs after applying CPN. According to [PU19], a good estimation for the this shift for MPE is

$$S_{\text{MPE}} = 2 \cdot \frac{\Theta}{n \cdot 360} \cdot h \quad (1)$$

The experiments performed in section 3 showed that by introducing pseudo perspectives, the vertical shift during comparison can be reduced by 50% to

$$S_{\text{PM-MPE}} = \frac{\Theta}{n \cdot 360} \cdot h \quad (2)$$

As indicated in [PKU19], a reduction of the shifts during comparison leads to lower scores in general, whereby the reduction of the impostor scores is higher than the one for genuine comparisons. This leads to a better separation of genuine and impostor scores, which in turn results in a better recognition rate.

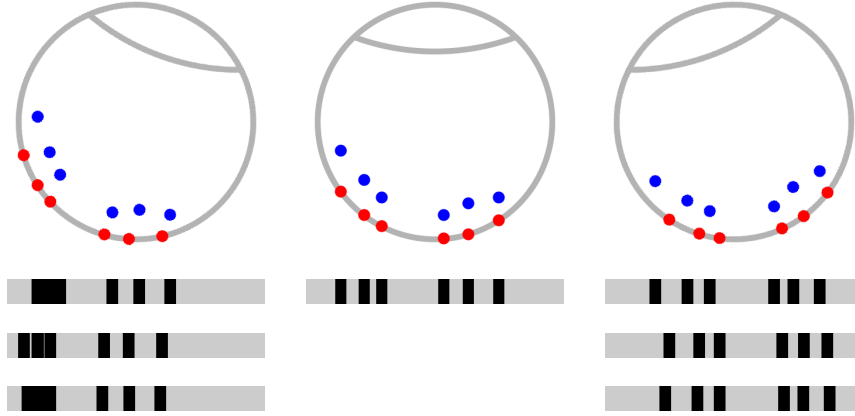


Fig. 2: Principle of pseudo perspective generation. Middle: cross section of a finger acquired during enrolment (top row). The blue points depict the veins inside the finger, the red points the veins projected on the skin surface of the finger. The bar below is the projected vein pattern. Left and right column: pseudo perspectives generated from the enrolment perspective. Top row: rotated versions of the finger ($\varphi = \pm 20^\circ$). Vein patterns: projection generated from the blue veins (top) and the red ones (middle), respectively. The bottom pattern is a shifted version of the blue vein pattern.

As mentioned above, the pseudo perspectives are generated by rotating the enrolment images by a defined angle of $\pm\varphi$. For an accurate rotation of the vein pattern, the position of the veins in the 2D image as well as the shape of the finger and the depth of the veins within the finger has to be known. As this information is not available in general, both need to be estimated. In this work it is assumed that a finger's cross section is approximately a circle (like Matsuda et al. assumed in [Ma16]) and that the imaged veins are located near to the skin surface [Hu10] and therefore can be assumed to be located on the skin surface. Fig. 2 depicts the principle of the generation of the additional perspectives for $\varphi = 20^\circ$. The image in the middle shows a schematic cross section of the finger in its position during enrolment. The blue dots represent the veins within the finger. The bar below is a projection of the vein pattern onto a 2D plain (representing the acquired vein pattern), where the black areas correspond to the veins. Before rotating the image for the perspective generation, the vein pattern is projected back onto the skin of the finger. The resulting vein position are visualized as red dots in the cross section. The left and right columns represent the generated pseudo perspectives, rotated by φ once to the left and once to the right. Since the projected veins (red dots) are located on the surface of the skin,

their position slightly deviates from that of the real veins (blue dots) in their true position after the rotation. As a result, also the vein patterns are slightly different. This deviation is illustrated by means of the vein patterns under the cross-section: the first pattern is the projection of the veins in its real position (blue dots), the second row the one of the rotated veins (red dots), respectively. The visually most noticeable difference between the two patterns is the horizontal shift. If they are aligned according to the highest correlation between them (as it is done with the Miura Matcher [MNM04] and visualized in the bottom row), the result is a high match. Please note that, although this explanation is done using vein patterns (feature space), the generation of the pseudo perspectives for PM-MPE is executed in the image space.

For the calculation of the pseudo perspectives, the position of a pixel within the ROI extracted from the enrolment image is defined by its x-coordinate x_{enrol} and the corresponding y-coordinate y_{enrol} , which is calculated by (3)

$$y_{enrol} = \sqrt{r^2 - x_{enrol}^2} \quad (3)$$

where r is the approximated radius of the finger. r is half the finger width, which corresponds to half of the height of the extracted finger ROI. The rotation for the pseudo perspective is calculated by applying the rotation matrix given in (4).

$$\begin{bmatrix} x_{pseudo} \\ y_{pseudo} \end{bmatrix} = \begin{bmatrix} \cos(-\varphi) & -\sin(-\varphi) \\ \sin(-\varphi) & \cos(-\varphi) \end{bmatrix} * \begin{bmatrix} x_{enrol} \\ y_{enrol} \end{bmatrix} \quad (4)$$

x_{pseudo} and y_{pseudo} are the coordinates of the vein pixel in the pseudo perspective and φ is the rotation angle. The actual image for the pseudo perspective is calculated from the grey values at x_{pseudo} using linear interpolation. Fig. 3 shows the ROIs (top row) and extracted MC features (bottom row) of an enrolled image (middle column) and its generated pseudo perspectives (left and right column). The pseudo perspectives are rotated versions of the enrolled image. The part of the pseudo perspectives that contain no information (due to the transform) is filled with the average grey level of the image.

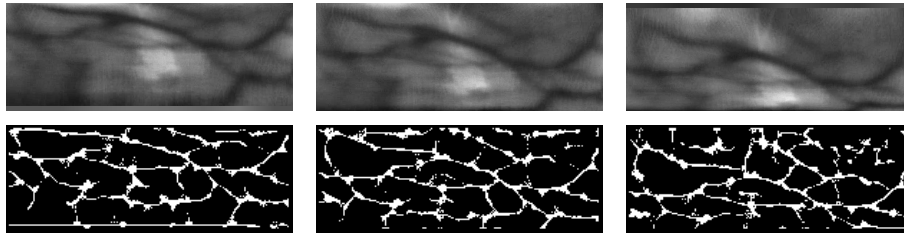


Fig. 3: ROI (top row) and extracted MC features (bottom row) of sample images of the PLUSVein-FR. Middle: enrolment image, left and right: generated pseudo perspectives for $\varphi = \pm 20^\circ$.

3 Experiments

In this section the results of the experiments carried out to evaluate the performance of the proposed PM-MPE approach are described. The method is analysed for different rotational distances between the acquired perspectives ($\alpha = 30^\circ, 45^\circ$ and 60°). Its results are compared to the results for MPE without perspective multiplication.

Data Set: The data set in use is the *PLUSVein Finger Rotation Data Set* (PLUSVein-FR). It has been acquired using a custom designed multi-perspective finger vein scanner that acquires finger vein images all around the finger (360°) with a resolution of 1° . It contains finger images captured from 63 different subjects, 4 fingers per subject, which sums up to a total of 252 unique fingers. Each finger is acquired 5 times. This results in 1.260 images per perspective. In this paper a subset containing perspectives in steps of 5° , resulting in 73 different perspectives (0° and 360° are acquired separately), is used. For more details on the data set the interested reader is referred to the authors previous publications [PKU18b, PKU18a].

Recognition Tool Chain: The finger vein recognition tool-chain consists of the following components: (1) For *finger region detection* and *finger alignment* an implementation that is based on [Lu13] is used. (2) The *ROI extraction* differs from [Lu13]: Instead of cutting out a defined rectangle within the finger, similar to [Hu10], a normalization of the finger to a fixed width is applied. (3) To improve the visibility of the vein pattern *Circular Gabor Filter* (CGF) [ZY09] and simple *CLAHE* (local histogram equalisation) [Zu94] are used during *pre-processing*. (4) As *feature extraction* method the well-established vein-pattern based *Maximum Curvature* (MC) method [MNM07] is employed. (5) The *comparison* of the binary feature images is done using a correlation measure, calculated between the input images and in x- and y-direction shifted and rotated versions of the reference image as described in [MNM04]. An implementation of the recognition tool-chain together with the used configurations and results are available for download on <http://wavelab.at/sources/Prommegger19e>.

Experimental Protocol: For the experiments, the data set is split into two subsets, one for enrolment and one for authentication. The enrolment subset contains two samples, the subset for authentication three samples. To quantify the performance, the EER, the FMR100 (the lowest FNMR for $FMR \leq 1\%$), the FMR1000 (the lowest FNMR for $FMR \leq 0,1\%$) as well as the ZeroFMR (the lowest FNMR for $FMR = 0\%$) are used. For the evaluation, the experiments follow the test protocol of the FVC2004 [Ma04]: For calculating the genuine scores, all possible genuine comparisons are performed, which are $63 \cdot 4 \cdot 3 \cdot 2 = 1512$ matches. For calculating the impostor scores, only the first image of a finger is compared against the first image of all other fingers, resulting in $(63 \cdot 4) \cdot (63 \cdot 4 - 1) = 63252$ matches, so together 64764 matches in total.

In order to have a reference for the quantification of MPE and PM-MPE results, the intra-perspective performance (IPP) of all 73 perspectives, without applying any rotation compensation methods and by applying CPN [PU19], is evaluated. For this calculations every perspective is considered as its own data set, which implies, that every perspective is its own independent classical single perspective recognition system where enrolment and probe image are acquired from the same perspective. As a result of this, rotational differences between the samples due to finger misplacement, i.e. longitudinal finger rotation, are subject to the same degradations as presented in [PKU18a]. Although the results of the different perspectives are presented together, they are completely independent from each other. Therefore, no rotational invariance can be concluded from the presentation of the intra-perspective results. As MPE and PM-MPE aim to generate rotation invariant recognition results for a single finger vein image acquired from any perspective during authentication, results close to or even better than the intra-perspective results without rotation correction can be considered as good performance.

Results: The left plot of Fig. 4 depicts the trend of the EER for MPE with rotational distances of $\alpha = 15^\circ, 30^\circ, 45^\circ$ and 60° and the intra-perspective performance results for applying no correction and CPN are visualized. Here MPE α means that the cameras for enrolment are positioned linearly spaced all around the finger (360°) with a rotational distance of α between two adjacent perspectives. For MPE 15° this results in $360/15 = 24$ cameras, for MPE 30° in $360/30 = 12$ cameras and so on. The best results for intra-perspective comparisons without rotation correction or applying CPN are obtained in the palmar region (0°) followed by the dorsal region (180°). The perspectives in-between show inferior results, achieving the worst results around 90° and 270° . CPN outperforms the results of no correction over the whole range in average by a factor of 2. MPE 15° and 30° clearly outperform the intra-perspective comparisons without rotation correction. This is reasonable since the PLUSVein-FR data set is, as all finger vein data sets, also subject to finger misplacements, e.g. longitudinal finger rotation, during its acquisition. By applying rotation correction or compensation methods, e.g. CPN, the negative effect on the recognition performance can be reduced. The results for MPE 45° are essentially the same as those of the intra-perspective comparisons without any rotation correction. MPE 60° delivers the worst results. Especially striking is the prominent performance degradation at 90° and 270° . There are two reasons for the bad performance in this regions: (1) As it can be seen from the intra-perspective evaluations, the performance in this region is generally inferior and (2) the distance to the acquired enrolment perspectives reaches its maximum. For MPE 60° , finger vein images are acquired at $0^\circ, 60^\circ, 120^\circ, 180^\circ, 240^\circ$ and 300° . For 90° and 270° this results in a rotational distance of 30° to the closest enrolment perspective. In [Pr19], the authors showed, that EPN, which is similar to the used CPN, cannot compensate such a high rotation. The simultaneous occurrence of both reasons explain the large performance drop to EERs of up to 20%.

The right plot of Fig. 4 shows the results for PM-MPE with rotational distances of $\alpha = 30^\circ, 45^\circ$ and 60° and the intra-perspective performance results applying no correction and CPN (note the different scaling compared to the MPE plot). α in PM-MPE α is again the rotational distance between two adjacent enrolment cameras. As described in section 2,

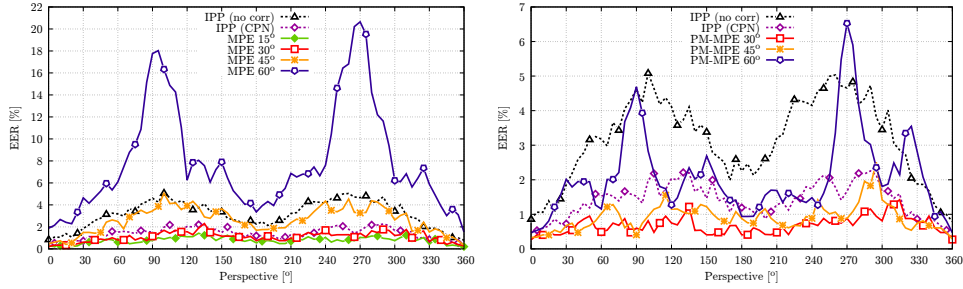


Fig. 4: Performance Results (EER) for MPE (left) and PM-MPE (right).

for PM-MPE the number of perspectives is tripled by generating pseudo perspectives of the acquired enrolment perspectives by rotating them with $\pm\varphi = 1/3\alpha$. PM-MPE 30° and PM-MPE 45° outperform the intra-perspective results showing a quite stable performance over the whole range from 0° to 360° with EERs below 2%. PM-MPE 60° exhibits the worst performance of the PM-MPE settings. The shape of the line shows that the performance for the perspectives degrades with the distance to the enrolment perspectives. This leads to a performance degradation around the perspectives that are farthest away from the enrolment perspectives, namely 30°, 90°, 150°, 210°, 270° and 330°. As for MPE 60°, the highest EER values are obtained around 90° and 270°. Except for the regions around 270° and 330°, PM-MPE 60° still outperforms the intra-perspective performance without correction.

Fig. 5 shows the trend of FMR100 and FMR1000 for both MPE and PM-MPE. FMR100 and FMR1000 follow the same trend as the EER in Fig. 4, just at a higher level.

For the comparison of the performance of MPE vs PM-MPE, the results of the two methods are shown side by side in Fig. 6. Each of the three subplots depicts the results for one rotational distance of the enrolment perspectives ($\alpha = 30^\circ, 45^\circ$ and 60°). They contain lines for MPE α , PM-MPE α and MPE ($\alpha-15^\circ$). Additionally, the results of the intra-perspective analysis without rotation correction and for applying CPN are added as references. One can see, that PM-MPE noticeably improves the robustness against longitudinal finger rotation. Multiplying the acquired enrolment perspectives always leads to an increase of the recognition performance compared to pure MPE with the same α . The experiments showed, that PM-MPE α even achieves recognition rates that are comparable to the ones of MPE with a 15° smaller α .

4 Conclusion

In this article, we introduced a method that effectively reduces the number of perspectives needed to be acquired during enrolment for MPE. The reduction is achieved by generating pseudo perspectives from the enrolled perspectives, captured in a rotational distance of

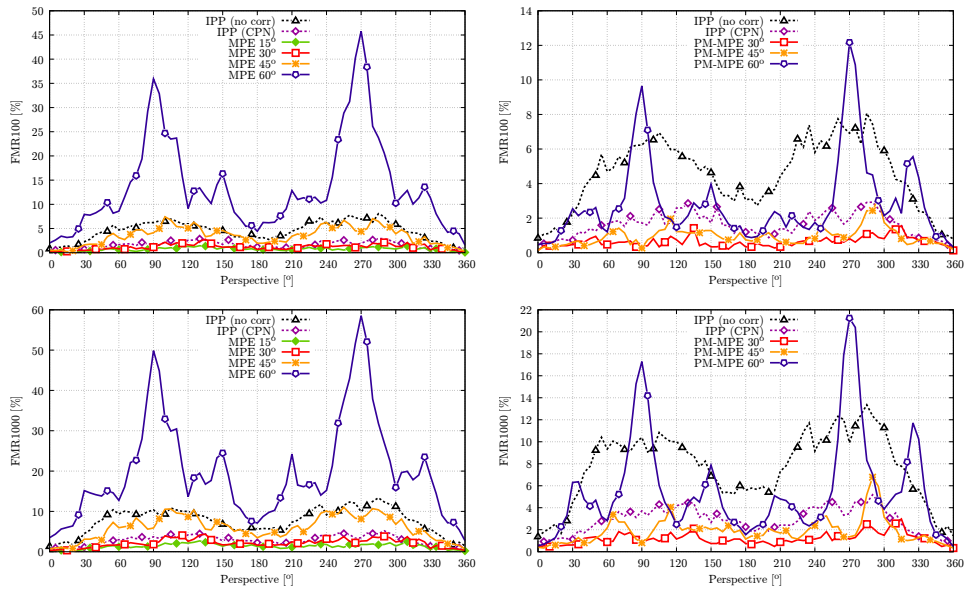


Fig. 5: Performance Results MPE (left) and PM-MPE (right): FMR100 (top) and FMR1000 (bottom).

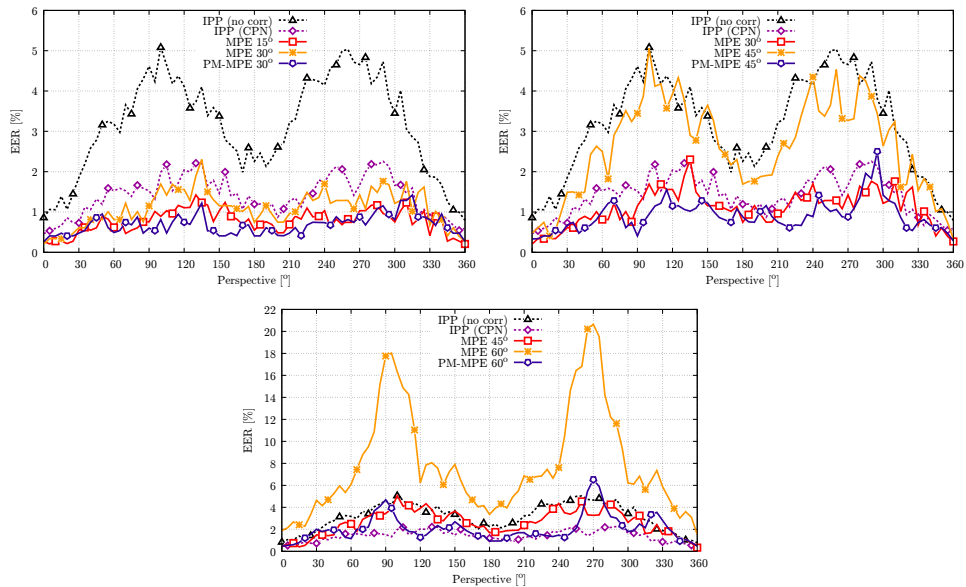


Fig. 6: Performance Results (EER) of MPE vs PM-MPE for a rotational distance of 30° (top-left), 45° (top-right) and 60° (bottom).

α , by rotating them with an angle of $\pm\varphi = \frac{1}{3}\alpha$. The obtained perspectives are used for additional comparisons during authentication.

The results showed that by applying PM-MPE, the rotational distance α between two enrolment perspectives can be increased by 15° while still getting comparable results. From MPE 15° to PM-MPE 30° this halves the number of cameras from 24 to 12, for 30° from 12 to 8 (reduction of $\frac{1}{3}$) and for 45° from 8 to 6 (reduction of $\frac{1}{4}$), respectively. A rotational distance of $\alpha > 60^\circ$ is neither useful for MPE, nor PM-MPE as currently available finger vein recognition systems are not able to compensate such high rotations. Reducing the number of perspectives acquired during enrolment reduces the cost and complexity of enrolment devices. Using PM-MPE on a limited range of e.g. $\pm 90^\circ$, would lead to enrolment devices with 3-4 cameras. Veldhuis *et al.* already presented a device that is capable of simultaneously acquiring 3 perspectives in [Ve19].

In our future work, we aim to further improve the performance (PM-)MPE and reduce the number of perspectives acquired during enrolment. Possible enhancements are a different positioning of the enrolment cameras (e.g. non-linear) or the generation of more than 2 pseudo perspectives between two adjacent enrolment perspectives. We also plan to evaluate MPE and PM-MPE for other recognition schemes than MC.

Acknowledgements

This work was supported in part by the European Union's Horizon 2020 Research and Innovation Program under Grant 700259, and in part by the FFG KIRAS Project AUTFingerATM under Grant 864785.

References

- [Ch18] Chen, Qing; Yang, Lu; Yang, Gongping; Yin, Yilong: Geometric shape analysis based finger vein deformation detection and correction. *Neurocomputing*, 2018.
- [Hu10] Huang, Beining; Dai, Yanggang; Li, Rongfeng; Tang, Darun; Li, Wenxin: Finger-vein authentication based on wide line detector and pattern normalization. In: *Pattern Recognition (ICPR), 2010 20th International Conference on*. IEEE, pp. 1269–1272, 2010.
- [KPU18] Kauba, Christof; Prommegger, Bernhard; Uhl, Andreas: The Two Sides of the Finger - An Evaluation on the Recognition Performance of Dorsal vs. Palmar Finger-Veins. In: *Proceedings of the International Conference of the Biometrics Special Interest Group (BIOSIG'18)*. Darmstadt, Germany, 2018.
- [KZ12] Kumar, Ajay; Zhou, Yingbo: Human identification using finger images. *Image Processing, IEEE Transactions on*, 21(4):2228–2244, 2012.
- [LLP09] Lee, Eui Chul; Lee, Hyeon Chang; Park, Kang Ryoung: Finger vein recognition using minutia-based alignment and local binary pattern-based feature extraction. *International Journal of Imaging Systems and Technology*, 19(3):179–186, 2009.
- [Lu13] Lu, Yu; Xie, Shan Juan; Yoon, Sook; Yang, Jucheng; Park, Dong Sun: Robust finger vein ROI localization based on flexible segmentation. *Sensors*, 13(11):14339–14366, 2013.

- [Ma04] Maio, Dario; Maltoni, Davide; Cappelli, Raffaele; Wayman, James L.; Jain, Anil K.: FVC2004: Third Fingerprint Verification Competition. In: ICBA. volume 3072 of LNCS. Springer Verlag, pp. 1–7, 2004.
- [Ma16] Matsuda, Yusuke; Miura, Naoto; Nagasaka, Akio; Kiyomiu, Harumi; Miyatake, Takafumi: Finger-vein authentication based on deformation-tolerant feature-point matching. *Machine Vision and Applications*, 27(2):237–250, 2016.
- [MNM04] Miura, Naoto; Nagasaka, Akio; Miyatake, Takafumi: Feature extraction of finger-vein patterns based on repeated line tracking and its application to personal identification. *Machine Vision and Applications*, 15(4):194–203, 2004.
- [MNM07] Miura, Naoto; Nagasaka, Akio; Miyatake, Takafumi: Extraction of finger-vein patterns using maximum curvature points in image profiles. *IEICE transactions on information and systems*, 90(8):1185–1194, 2007.
- [PKU18a] Prommegger, Bernhard; Kauba, Christof; Uhl, Andreas: Longitudinal Finger Rotation - Problems and Effects in Finger-Vein Recognition. In: Proceedings of the International Conference of the Biometrics Special Interest Group (BIOSIG'18). Darmstadt, Germany, 2018.
- [PKU18b] Prommegger, Bernhard; Kauba, Christof; Uhl, Andreas: Multi-Perspective Finger-Vein Biometrics. In: Proceedings of the IEEE 9th International Conference on Biometrics: Theory, Applications, and Systems (BTAS2018). Los Angeles, California, USA, 2018.
- [PKU19] Prommegger, Bernhard; Kauba, Christof; Uhl, Andreas: On the Extent of Longitudinal Finger Rotation in Publicly Available Finger Vein Data Sets. In: Proceedings of the 12th IAPR/IEEE International Conference on Biometrics (ICB'19). Crete, Greece, pp. 1–8, 2019.
- [Pr19] Prommegger, Bernhard; Kauba, Christof; Linortner, Michael; Uhl, Andreas: Longitudinal Finger Rotation - Deformation Detection and Correction. *IEEE Transactions on Biometrics, Behavior, and Identity Science*, 1(2):123–138, 2019.
- [PU19] Prommegger, Bernhard; Uhl, Andreas: Rotation Invariant Finger Vein Recognition. In: Proceedings of the IEEE 10th International Conference on Biometrics: Theory, Applications, and Systems (BTAS2019). Tampa, Florida, USA, 2019.
- [Ve19] Veldhuis, Raymond; Spreeuwens, Luuk; Ton, Bram; Rozendal, Sjoerd: A high quality finger vein dataset collected using a custom designed capture device. In (Uhl, Andreas; Busch, Christoph; Marcel, Sebastien; Veldhuis, Raymond, eds): *Handbook of Vascular Biometrics*, chapter 5, p. 13 pages. Springer Science+Business Media, Boston, MA, USA, 2019.
- [Ya17] Yang, Lu; Yang, Gongping; Yin, Yilong; Xi, Xiaoming: Finger Vein Recognition with Anatomy Structure Analysis. *IEEE Transactions on Circuits and Systems for Video Technology*, pp. 1–1, 2017.
- [Zu94] Zuiderveld, K.: Contrast Limited Adaptive Histogram Equalization. In (Heckbert, Paul S., ed.): *Graphics Gems IV*, pp. 474–485. Morgan Kaufmann, 1994.
- [ZY09] Zhang, Jing; Yang, Jinfeng: Finger-vein image enhancement based on combination of gray-level grouping and circular Gabor filter. In: *Information Engineering and Computer Science*, 2009. ICIECS 2009. International Conference on. IEEE, pp. 1–4, 2009.